

Reevaluating Reactor Antineutrino Anomalies with Updated Flux Predictions

Jeffrey M. Berryman^{1,2,3} and Patrick Huber¹

¹*Center for Neutrino Physics, Department of Physics, Virginia Tech, Blacksburg, VA 24061, USA*

²*Department of Physics and Astronomy, University of Kentucky, Lexington, KY 40506, USA*

³*Department of Physics, University of California, Berkeley, CA 94720, USA*

Hints for the existence of a sterile neutrino at nuclear reactors are reexamined using two updated predictions for the fluxes of antineutrinos produced in fissions. These new predictions diverge in their preference for the rate deficit anomaly, relative to previous analyses, but the anomaly in the ratios of measured antineutrino spectra persists. We comment on upcoming experiments and their ability to probe the preferred region of the sterile-neutrino parameter space in the electron neutrino disappearance channel.

Introduction: The evidence for the existence of additional neutrino species, which we generically call “sterile neutrinos,” can be broadly decomposed into three classes: anomalous $\bar{\nu}_e$ disappearance at reactors [1]; anomalous ν_e disappearance at GALLEX [2] and SAGE [3], i.e., the gallium anomaly; and anomalous $\bar{\nu}_e$ appearance at LSND [4] and MiniBooNE [5]. These individual pieces, however, do not form a consistent whole. The reactor and gallium anomalies were found to be compatible at only the 9% level in Ref. [6]. Moreover, the combination of these and the absence of anomalous $\nu_\mu/\bar{\nu}_\mu$ disappearance is incongruous with the LSND and MiniBooNE appearance anomalies. For recent reviews on the status of light sterile neutrinos, see Refs. [7, 8].

It is natural to consider, then, why this picture breaks down. While models of new physics have been proposed to explain these anomalies [9–16], an obvious starting point is to scrutinize each to establish how robust it really is. Regarding the gallium anomaly, the $^{69,71}\text{Ga}(\nu_e, e^-)^{69,71}\text{Ge}$ cross sections have recently been reevaluated in Ref. [17] using an updated shell-model calculation. The preference for a sterile neutrino is weaker than for previous calculations, but the compatibility between the gallium and reactor anomalies is improved to 16% [17]. On the other hand, the LSND and MiniBooNE anomalies will be extensively probed by the upcoming short-baseline program at Fermilab [18, 19]. In this letter, we focus on the the electron neutrino *disappearance* channel.

We have reevaluated the reactor antineutrino anomaly (RAA) using updated predictions for the reactor antineutrino fluxes. The RAA is comprised of two parts: a deficit in the observed number of $\bar{\nu}_e$ interactions relative to predictions and the existence of features in measured $\bar{\nu}_e$ spectral ratios. We address both of these in what follows. Our results are obtained with the publicly available software GLOBES [20, 21]; the underlying data libraries used to produce our results will be published in an accompanying software paper [22].

Updated Flux Predictions: Over the past decade, the Huber-Mueller (HM) $\bar{\nu}_e$ flux predictions [23, 24] have been the standard fluxes for calculations at reactors. These are derived from measurements of the aggregate β spectra from the products of nuclear fissions [25–27].

These β spectra are then converted to obtain predictions for the corresponding $\bar{\nu}_e$ spectra using virtual β branches; see Refs. [23, 24] for details. While the physics that enters into this procedure is broadly well understood, we highlight two sources of systematic uncertainty. (1) *The accuracy of the underlying data.* It cannot be excluded that there may be unaccounted-for systematics in the measurements of aggregate β spectra that bias the results. (2) *The theoretical understanding of the component β decays.* The conversion procedure assumes that all β decays are of allowed type. However, a large fraction – up to 40% – of all decays are so-called forbidden decays. This introduces large uncertainties related to nuclear structure.

An alternative to the conversion method exists in the *ab initio* method. Here, one adds the spectra from every accessible β branch of every fission fragment, with appropriate weights determined by the cumulative fission fraction of each isotope, to determine the overall β spectrum. This method benefits from using *physical* β branches in lieu of *virtual* branches and thus can avoid some of the approximations made in the conversion method. However, this technique is similarly reliant on experimental data, both for the strengths of the individual β branches and for the fission yields, which have historically been lacking. In recent years, the beta feeding data have been revisited and improved using Total Absorption Gamma Spectroscopy (TAGS), see *e.g.* [28]. Furthermore, *ab initio* calculations are also dependent on a theoretical understanding of forbidden decays.

Two new antineutrino flux predictions have recently appeared in the literature. An updated *ab initio* calculation was recently published in Ref. [28]. There, it was found that *ab initio* predictions produce better agreement with the $\bar{\nu}_e$ spectrum measured at Daya Bay than the HM predictions. This is due, in large part, to a $\sim 10\%$ reduction in the flux from ^{235}U , a feature that is consistent with previous findings [29, 30]. The improvement largely stems from the improved β spectrum feeding functions obtained from TAGS measurements. However, these calculations do not go beyond the allowed approximation.

An updated conversion method calculation has been presented in Ref. [31]; we refer to this calculation as “HKSS” in the remainder of this work. The significant

improvement in HKSS is that forbidden decays are including via nuclear shell model calculations to describe the underlying microscopic physics, allowing the authors to derive the relevant shape factors. The authors find an unspecific enhancement of the antineutrino flux at energies above 4 MeV relative to HM, mitigating somewhat the size of the infamous 5 MeV bump [30, 32–34] and increasing the predicted antineutrino flux.

We have considered the impact of all three of these flux predictions on the preference of the global reactor antineutrino data set for a sterile neutrino. An important factor in these analyses is the size of the theoretical uncertainties on the flux predictions. The HKSS flux predictions are published with uncertainties; see the appendix to Ref. [31]. In our calculations, we use the uncertainties from their parameterized results. The *ab initio* fluxes, however, have no stated uncertainties. In the absence of a more compelling option, we assign the fractional uncertainties on the HM predictions to the *ab initio* predictions in our analysis. This is an optimistic assignment of uncertainties; we will argue, however, that this does not affect the conclusions of this work.

The Rate Anomaly: We begin with combined analyses of the inverse beta decay (IBD) event rates measured at the short-baseline experiments at Bugey [35, 36], Gösgen [37], ILL [38, 39], Krasnoyarsk [40–42], Nucifer [43], Savannah River [44] and Rovno [45, 46]. Additionally, we analyze Chooz [47], Double Chooz [34] and Palo Verde [48, 49] at medium baselines, as well as fuel evolution results from Daya Bay [50] and RENO [51, 52]. We highlight the salient features of our analysis here; see Ref. [22] for more details.

Our analysis is constructed using ratios of the IBD rates measured at these experiments relative to the three-neutrino predictions for the three reactor antineutrino flux models mentioned previously. We use GLOBES to calculate the total event rate at each experiment as a function of two sterile-neutrino parameters – the effective mixing angle $\sin^2 2\theta_{ee}$ and the mass-squared splitting Δm_{41}^2 . For short-baseline experiments, we use the two-flavor approximation for the survival probability,

$$P_{ee} \approx 1 - \sin^2 2\theta_{ee} \sin^2 \left(\frac{\Delta m_{41}^2 L}{4E_\nu} \right). \quad (1)$$

For the medium-baseline experiments, we use the full four-flavor oscillation formalism with the best-fit values for the usual three-neutrino oscillation parameters from Ref. [53].*

The differences between the experimental and predicted ratios are combined into a global χ^2 function,

$$\chi^2 = (\vec{R}_{\text{exp}} - \vec{R}_{\text{pred}})^T \cdot V_{\text{exp}}^{-1} \cdot (\vec{R}_{\text{exp}} - \vec{R}_{\text{pred}}) + \vec{\xi}^T \cdot V_{\text{th}}^{-1} \cdot \vec{\xi}, \quad (2)$$

* We assume that the existence of a sterile neutrino has not caused any of these parameters to be mismeasured.

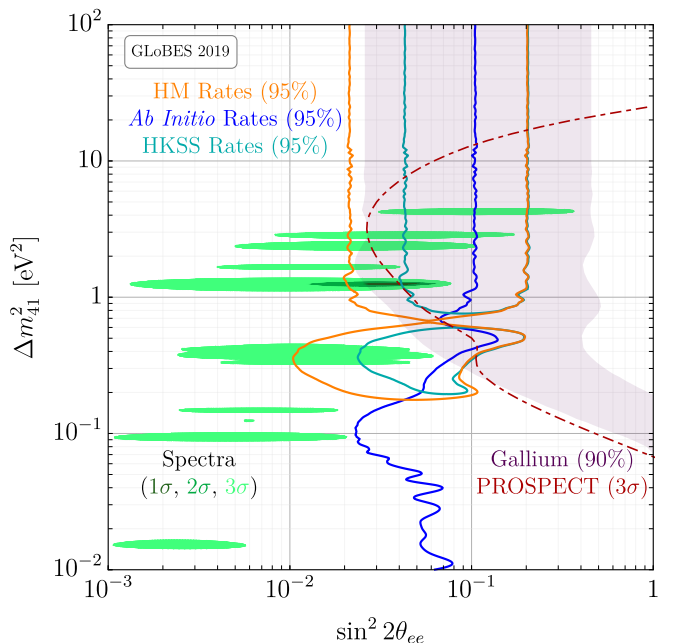


FIG. 1. The 95% C.L. contours from IBD rate measurements using the HM (orange), *ab initio* (blue) and HKSS (dark cyan) flux predictions. The regions preferred by reactor antineutrino spectra at 1σ , 2σ and 3σ are shown in light, medium and dark green, respectively. We show the 90% C.L. region preferred by the gallium anomaly [17], for comparison. The red, dot-dashed curve shows the 3σ sensitivity of PROSPECT [54] assuming three years of operation.

where \vec{R}_{exp} is the vector of experimental ratios, $\vec{R}_{\text{pred}} = \vec{R}_{\text{pred}}(\sin^2 2\theta_{ee}, \Delta m_{41}^2, \vec{\xi})$ is the vector of predicted ratios and $\vec{\xi}$ is a vector of nuisance parameters describing the normalization uncertainties on the isotopic flux predictions – one each for ^{235}U , ^{238}U , ^{239}Pu and ^{241}Pu . Further, V_{exp} is the covariance matrix describing experimental uncertainties, including correlations, and V_{th} is the covariance matrix for $\vec{\xi}$. We minimize over the $\vec{\xi}$ for each point in $\sin^2 2\theta_{ee}$ – Δm_{41}^2 parameter space.

We cross-check our results with the HM flux model against the *rate* results in Refs. [1, 6, 55–58]. We find general good agreement; the resulting 95% C.L. curve is shown in orange in Fig. 1. The HM fluxes are then replaced in favor of the *ab initio* and HKSS fluxes and the analysis is repeated; the resulting 95% C.L. curves are shown, respectively, in blue and dark cyan in Fig. 1. For context, we show the region preferred by the gallium anomaly at 90% C.L. [17] in shaded purple.

The updated flux models diverge, relative to the HM fluxes, in their preference for a sterile neutrino. On one hand, the *ab initio* fluxes indicate a much *weaker* preference for a sterile neutrino; these fluxes prefer nonzero mixing at $< 1\sigma$. This can be largely attributed to the reduced total flux from ^{235}U fissions relative to the HM predictions, as mentioned above. Further, recall that assigning the HM uncertainties to the *ab initio* fluxes un-

Analysis	$\chi_{3\nu}^2$	χ_{\min}^2	n_{data}	p	$n\sigma$
HM Rates	41.4	33.5	40	2.0×10^{-2}	2.3
<i>Ab Initio</i> Rates	39.2	37.0	40	0.34	0.95
HKSS Rates	58.1	47.5	40	5.0×10^{-3}	2.8
Spectra	184.9	172.2	212	1.8×10^{-3}	3.1
DANSS + NEOS	98.9	84.7	84	8.1×10^{-4}	3.3

TABLE I. A summary of relevant statistics in our analyses. We show χ^2 for $\sin^2 2\theta_{ee} = 0$, $\chi_{3\nu}^2$, and the minimum value of χ^2 over the sterile neutrino parameter space, χ_{\min}^2 . We also tabulate the number of data points for each analysis, n_{data} , the p -value at which three-neutrino mixing can be excluded and the number of σ corresponding to that p -value.

derestimates the true theoretical uncertainty. A more realistic error budget would further degrade the preference for a sterile neutrino. On the other hand, the HKSS predictions result in *stronger* evidence for a sterile neutrino: recalculating the shape factor accounting for forbidden decays results in an increased expected IBD rate, implying larger experimental deficits. Relevant statistics for these analyses are compiled in Table I.

We conclude this discussion by underscoring that the diverging preference for a sterile neutrino between the *ab initio* and HKSS flux predictions highlights the need to reappraise the data underpinning these predictions. As of present, improved TAGS measurements in the *ab initio* model and the more complete treatment of forbidden decays in HKSS modify the total predicted rate to roughly the same degree but with opposite signs. Concerns about vastly increased uncertainties from first-forbidden decays [59] seem not to be borne out in the detailed analysis in HKSS. That said, these conclusions can only be solidified with the collection of more and improved data.

The Spectral Anomaly: We shift our attention to the reactor $\bar{\nu}_e$ energy spectra measured at Bugey [36], DANSS [60], Daya Bay [61], Double Chooz [34], NEOS [32] and RENO [33]. With the exception of NEOS, each of these experiments measures the $\bar{\nu}_e$ spectrum at multiple positions and publishes ratios of these spectra. The benefit of such ratios is that the dependence on the reactor flux model largely cancels, mitigating theoretical uncertainties. The NEOS collaboration presents their spectrum as a ratio with respect to the spectrum measured at Daya Bay in Ref. [62], which introduces mild flux model dependence into the analysis; see Ref. [22] for details.

PROSPECT [63] and STEREO [64, 65] have also produced constraints in the last few years. Given that these experiments are still collecting data and that only limited information on how to include them in a global fit is available, we choose not to include them here. We discuss their expected impact below.

The two-flavor approximation in Eq. (1) is used for Bugey, DANSS and NEOS, but we use the full four-neutrino framework for Daya Bay, Double Chooz and RENO. These spectral ratios are combined in a single

χ^2 function of the form

$$\chi^2 = \sum_A (\vec{S}_{\text{exp}}^A - \vec{S}_{\text{pred}}^A)^T \cdot (V_A)^{-1} \cdot (\vec{S}_{\text{exp}}^A - \vec{S}_{\text{pred}}^A), \quad (3)$$

where A indexes the experiments, \vec{S}_{exp}^A is the experimental spectral ratio and $\vec{S}_{\text{pred}}^A = \vec{S}_{\text{pred}}^A(\sin^2 2\theta_{ee}, \Delta m_{41}^2)$ is the predicted spectral ratio. Each experiment has its own covariance matrix V_A that includes both experimental and theoretical uncertainties. In principle, all experiments are correlated through the theoretical uncertainties. Practically speaking, these correlations are negligible.

The χ^2 is calculated at each point in the $\sin^2 2\theta_{ee} - \Delta m_{41}^2$ parameter space; the results are shown in Fig. 1. The 1σ , 2σ and 3σ preferred regions are shown in dark, medium and light green, respectively, and are consistent with similar results in Refs. [6, 29, 57]. The sensitivity is primarily driven by DANSS; the total evidence for a sterile neutrino is 3.1σ . It is noteworthy that NEOS and DANSS point to the same Δm_{41}^2 despite their baselines differing by a factor of two. Relevant statistics are compiled in the last line of Tab. I.

We do not combine our rate and spectral analyses; there are nontrivial correlations between the rate measurements at Bugey, Daya Bay, Double Chooz and RENO and the corresponding spectral measurements that would need to be taken into account. However, one can infer from Fig. 1 that the spectral analysis is consistent with the *ab initio* analysis; the latter shows weak preference for a sterile neutrino, so consistency is essentially guaranteed. However, one can also infer that the tension between the spectral and HKSS analysis is greater than with the HM analysis. In this way, too, we see the *ab initio* and HKSS analyses diverge.

Future Experiments: It is useful and imperative to consider how this parameter space can be probed in the near term, given the uncertainty surrounding analyses of the rates but the apparent robustness of spectral measurements. We consider only experiments searching for $\nu_e/\bar{\nu}_e$ disappearance; for discussions on the future of $\nu_e/\bar{\nu}_e$ appearance and $\nu_\mu/\bar{\nu}_\mu$ appearance/disappearance, see Refs. [7, 8].

We begin with PROSPECT and STEREO, which have produced early results [63–65], but not, at present, final analyses. These experiments were designed in the first half of the decade to conclusively probe the RAA as presented in Ref. [1]; early results indicate that they will achieve this. However, since these experiments were conceived, reactor spectrum experiments have shifted the preferred sterile neutrino parameters to smaller mixing angles than previously indicated.

We use PROSPECT as proxy to study how well current-generation reactor can probe the regions preferred by the four global analyses presented here. The expected 3σ sensitivity for three years of operation is shown in dot-dashed dark red in Fig. 1 [54]. This sensitivity represent a prediction of how a null result from

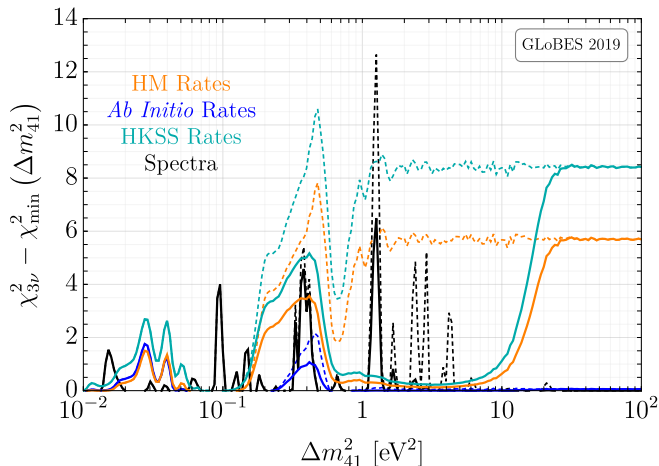


FIG. 2. The difference between the three-neutrino χ^2 , $\chi_{3\nu}^2$, and the minimum four-neutrino χ^2 for a fixed Δm_{41}^2 , $\chi_{\min}^2(\Delta m_{41}^2)$. The dashed lines are for the four global analyses presented here: HM rates (orange), *ab initio* rates (blue), HKSS rates (dark cyan) and spectra (black); the solid lines show the remaining preference for oscillation after the inclusion of a hypothetical null result from PROSPECT.

PROSPECT, *i.e.* no evidence for oscillation, would constrain the parameter space. The question then is, how much of the currently allowed regions would survive? To quantify this, we calculate the difference between the three-neutrino χ^2 , $\chi_{3\nu}^2$, and the minimum four-neutrino χ^2 for fixed Δm_{41}^2 , $\chi_{\min}^2(\Delta m_{41}^2)$ – a measure of the preference the data show for oscillation at a given Δm_{41}^2 – for each analysis presented here. Specifically, we consider how a null result from PROSPECT would reduce this quantity and hence, how much the allowed parameter space is reduced.

The results are shown in Fig. 2. The dashed curves show $\chi_{3\nu}^2 - \chi_{\min}^2(\Delta m_{41}^2)$ for the HM rates (orange), *ab initio* rates (blue), HKSS rates (dark cyan) and spectra (black) analyses with no contribution from PROSPECT. The solid curves are similar, except PROSPECT’s sensitivity has been folded in. In regions where the difference between the dashed and solid curves of a given color is large, PROSPECT reduces the allowed parameter space significantly. PROSPECT is effective at probing the HM and HKSS rate analyses in the region $\Delta m_{41}^2 \sim 1 - 10 \text{ eV}^2$; this is precisely the region of parameter space for which it was designed. Conversely, PROSPECT does little to challenge the *ab initio* rate analysis, since this produces weak preference for a sterile neutrino in the first place.

Most interesting is its sensitivity to the spectral anomaly. Measurements of spectral ratios are susceptible to statistical fluctuations that ensure a best-fit point at nonzero mixing; see Ref. [66] for more discussion. The precise 1σ and 2σ preferred regions might be the result of such fluctuations, but the 3σ preferred region is less likely to be influenced by these. Consequently, we advocate taking a broader view of the preferred parameter

space when considering the impact of PROSPECT on the spectral anomaly. PROSPECT is strongest in probing the region $\Delta m_{41}^2 \sim 1 - 5 \text{ eV}^2$, similar to the HM and HKSS analyses. However, it only has modest power to probe the region $\Delta m_{41}^2 \sim 0.1 - 0.5$, where the preference for a sterile neutrino is also nontrivial. Overall, a 2.4σ preference for oscillation would remain even after a null result from PROSPECT.

IsoDAR [67], which is a proposal to use a high-intensity $\bar{\nu}_e$ source from β decays of ${}^8\text{Li}$, has a expected 5σ sensitivity [7] that suggests it has the potential to emphatically confirm or refute the sterile-neutrino interpretation of the RAA. There also exists a burgeoning program of experiments searching for coherent elastic neutrino-nucleus scattering [68–77] that may be able to probe the anomaly [78, 79] at high significance, though this process has not yet been observed at a nuclear reactor.

Conclusions: We have reanalyzed the global reactor $\bar{\nu}_e$ data set using three reactor antineutrino flux predictions. Relative to the traditional HM predictions, the two new calculations result in diverging evidence for a sterile neutrino when total IBD rate measurements are considered – the *ab initio* calculation decreases the significance from 2.3σ to 0.95σ , whereas the HKSS calculation increases the significance to 2.8σ . However, the spectral anomaly is robust with respect to varying the flux model and is found to persist at the 3.1σ level. We have briefly reviewed the capabilities of current searches for sterile neutrinos – PROSPECT, in particular – to cover the parameter space preferred by each of these four analyses and find that a significant fraction of parameter space would remain even for a null result in those searches.

We are aware of the optics of the current situation: the region of parameter space preferred by the spectral anomaly lies *just* beyond the reach of past and current experiments. However, this feature is shared with genuine discoveries; for example, θ_{13} was just beyond the sensitivity of the Chooz experiment. We have shown that null results from current reactor experiments would leave a significant fraction of the currently favored parameter space unexplored. Furthermore, the data in the electron disappearance channel are self-consistent, irrespective of the flux model used. Proclamations of the demise of the light sterile neutrino are, therefore, premature.

Given the current evidence for the existence of light sterile neutrinos, it is crucial that the next generation of oscillation experiments includes an effective strategy for probing the sterile neutrino hypothesis in the electron neutrino disappearance channel.

Acknowledgments: We thank Giorgio Gratta (Palo Verde); Soo-Bong Kim (RENO); David Lhuillier (STEREO); and Karsten Heeger, Bryce Littlejohn and Pranava Teja Surukuchi (PROSPECT) for providing data and useful discussions. We also thank Muriel Fallot for providing the *ab initio* fluxes in machine-readable format and Leendert Hayen for information on the HKSS model. JMB thanks the Fermilab Theory Division for their hospitality during the completion of this work. This

work is supported by DOE Office of Science awards [de-sc0018327](#) and [de-sc0020262](#). The work of JMB is also

supported by NSF Grant PHY-1630782 and by Heising-Simons Foundation Grant 2017-228.

-
- [1] G. Mention, M. Fechner, Th. Lasserre, Th. A. Mueller, D. Lhuillier, M. Cribier, and A. Letourneau, “The Reactor Antineutrino Anomaly,” *Phys. Rev.* **D83**, 073006 (2011), 1101.2755.
- [2] W. Hampel et al. (GALLEX), “Final results of the ^{51}Cr neutrino source experiments in GALLEX,” *Phys. Lett.* **B420**, 114 (1998).
- [3] J. N. Abdurashitov et al. (SAGE), “Measurement of the response of the Russian-American gallium experiment to neutrinos from a ^{51}Cr source,” *Phys. Rev.* **C59**, 2246 (1999), hep-ph/9803418.
- [4] A. Aguilar-Arevalo et al. (LSND), “Evidence for neutrino oscillations from the observation of $\bar{\nu}_e$ appearance in a $\bar{\nu}_\mu$ beam,” *Phys. Rev.* **D64**, 112007 (2001), hep-ex/0104049.
- [5] A. A. Aguilar-Arevalo et al. (MiniBooNE), “Improved Search for $\bar{\nu}_\mu \rightarrow \bar{\nu}_e$ Oscillations in the MiniBooNE Experiment,” *Phys. Rev. Lett.* **110**, 161801 (2013), 1303.2588.
- [6] M. Dentler, A. Hernández-Cabezudo, J. Kopp, P. A. N. Machado, M. Maltoni, I. Martinez-Soler, and T. Schwetz, “Updated Global Analysis of Neutrino Oscillations in the Presence of eV-Scale Sterile Neutrinos,” *JHEP* **08**, 010 (2018), 1803.10661.
- [7] A. Diaz, C. A. Argüelles, G. H. Collin, J. M. Conrad, and M. H. Shaevitz, “Where Are We With Light Sterile Neutrinos?,” (2019), 1906.00045.
- [8] S. Böser, C. Buck, C. Giunti, J. Lesgourgues, L. Ludhova, S. Mertens, A. Schukraft, and M. Wurm, “Status of Light Sterile Neutrino Searches,” (2019), 1906.01739.
- [9] A. Merle, S. Morisi, and W. Winter, “Common origin of reactor and sterile neutrino mixing,” *JHEP* **07**, 039 (2014), 1402.6332.
- [10] P. Bakhti, Y. Farzan, and T. Schwetz, “Revisiting the quantum decoherence scenario as an explanation for the LSND anomaly,” *JHEP* **05**, 007 (2015), 1503.05374.
- [11] K. S. Babu, D. W. McKay, I. Mocioiu, and S. Pakvasa, “Light sterile neutrinos, lepton number violating interactions, and the LSND neutrino anomaly,” *Phys. Rev.* **D93**, 113019 (2016), 1605.03625.
- [12] M. Carena, Y.-Y. Li, C. S. Machado, P. A. N. Machado, and C. E. M. Wagner, “Neutrinos in Large Extra Dimensions and Short-Baseline ν_e Appearance,” *Phys. Rev.* **D96**, 095014 (2017), 1708.09548.
- [13] G. Magill, R. Plestid, M. Pospelov, and Y.-D. Tsai, “Dipole Portal to Heavy Neutral Leptons,” *Phys. Rev.* **D98**, 115015 (2018), 1803.03262.
- [14] D. Döring, H. Päs, P. Sicking, and T. J. Weiler, “Sterile Neutrinos with Altered Dispersion Relations as an Explanation for the MiniBooNE, LSND, Gallium and Reactor Anomalies,” (2018), 1808.07460.
- [15] J. Liao, D. Marfatia, and K. Whisnant, “MiniBooNE, MINOS+ and IceCube data imply a baroque neutrino sector,” *Phys. Rev.* **D99**, 015016 (2019), 1810.01000.
- [16] P. B. Denton, Y. Farzan, and I. M. Shoemaker, “Activating the fourth neutrino of the 3+1 scheme,” *Phys. Rev.* **D99**, 035003 (2019), 1811.01310.
- [17] J. Kostensalo, J. Suhonen, C. Giunti, and P. C. Srivastava, “The gallium anomaly revisited,” *Phys. Lett.* **B795**, 542 (2019), 1906.10980.
- [18] M. Antonello et al. (MicroBooNE, LAr1-ND, ICARUS-WA104), “A Proposal for a Three Detector Short-Baseline Neutrino Oscillation Program in the Fermilab Booster Neutrino Beam,” (2015), 1503.01520.
- [19] P. A. Machado, O. Palamara, and D. W. Schmitz, “The Short-Baseline Neutrino Program at Fermilab,” *Ann. Rev. Nucl. Part. Sci.* **69** (2019), 1903.04608.
- [20] P. Huber, M. Lindner, and W. Winter, “Simulation of long-baseline neutrino oscillation experiments with GLOBES (General Long Baseline Experiment Simulator),” *Comput. Phys. Commun.* **167**, 195 (2005), hep-ph/0407333.
- [21] P. Huber, J. Kopp, M. Lindner, M. Rolinec, and W. Winter, “New features in the simulation of neutrino oscillation experiments with GLOBES 3.0: General Long Baseline Experiment Simulator,” *Comput. Phys. Commun.* **177**, 432 (2007), hep-ph/0701187.
- [22] J. M. Berryman and P. Huber, in Preparation.
- [23] Th. A. Mueller et al., “Improved Predictions of Reactor Antineutrino Spectra,” *Phys. Rev.* **C83**, 054615 (2011), 1101.2663.
- [24] P. Huber, “On the determination of anti-neutrino spectra from nuclear reactors,” *Phys. Rev.* **C84**, 024617 (2011), [Erratum: *Phys. Rev.* **C85**, 029901 (2012)], 1106.0687.
- [25] F. Von Feilitzsch, A. A. Hahn, and K. Schreckenbach, “Experimental beta-spectra from ^{239}Pu and ^{235}U thermal neutron fission products and their correlated antineutrino spectra,” *Phys. Lett.* **118B**, 162 (1982).
- [26] K. Schreckenbach, G. Colvin, W. Gelletly, and F. Von Feilitzsch, “Determination of the antineutrino spectrum from ^{235}U thermal neutron fission products up to 9.5 MeV,” *Phys. Lett.* **160B**, 325 (1985).
- [27] A. A. Hahn, K. Schreckenbach, G. Colvin, B. Krusche, W. Gelletly, and F. Von Feilitzsch, “Antineutrino spectra from ^{241}Pu and ^{239}Pu thermal neutron fission products,” *Phys. Lett.* **B218**, 365 (1989).
- [28] M. Estienne et al., “Updated Summation Model: An Improved Agreement with the Daya Bay Antineutrino Fluxes,” *Phys. Rev. Lett.* **123**, 022502 (2019), 1904.09358.
- [29] S. Gariazzo, C. Giunti, M. Laveder, and Y. F. Li, “Model-independent $\bar{\nu}_e$ short-baseline oscillations from reactor spectral ratios,” *Phys. Lett.* **B782**, 13 (2018), 1801.06467.
- [30] D. Adey et al. (Daya Bay), “Measurement of Individual Antineutrino Spectra from ^{235}U and ^{239}Pu at Daya Bay,” (2019), 1904.07812.
- [31] L. Hayen, J. Kostensalo, N. Severijns, and J. Suhonen, “First-forbidden transitions in the reactor anomaly,” (2019), 1908.08302.
- [32] Y. Ko et al. (NEOS), “Sterile Neutrino Search at the NEOS Experiment,” *Phys. Rev. Lett.* **118**, 121802 (2017), 1610.05134.
- [33] G. Bak et al. (RENO), “Measurement of Reactor Antineutrino Oscillation Amplitude and Frequency

- at RENO,” *Phys. Rev. Lett.* **121**, 201801 (2018), 1806.00248.
- [34] H. De Kerret et al. (Double Chooz), “First Double Chooz θ_{13} Measurement via Total Neutron Capture Detection,” (2019), 1901.09445.
- [35] Y. Declais et al., “Study of reactor anti-neutrino interaction with proton at Bugey nuclear power plant,” *Phys. Lett.* **B338**, 383 (1994).
- [36] Y. Declais et al., “Search for neutrino oscillations at 15-meters, 40-meters, and 95-meters from a nuclear power reactor at Bugey,” *Nucl. Phys.* **B434**, 503 (1995).
- [37] G. Zacek et al. (CALTECH-SIN-TUM), “Neutrino Oscillation Experiments at the Gösigen Nuclear Power Reactor,” *Phys. Rev.* **D34**, 2621 (1986).
- [38] H. Kwon, F. Boehm, A. A. Hahn, H. E. Henrikson, J. L. Vuilleumier, J. F. Cavaignac, D. H. Koang, B. Vignon, F. Von Feilitzsch, and R. L. Mossbauer, “Search for Neutrino Oscillations at a Fission Reactor,” *Phys. Rev.* **D24**, 1097 (1981).
- [39] A. Hoummada, S. Lazrak Mikou, M. Avenier, G. Bagieu, J. F. Cavaignac, and Dy. Holm Koan, “Neutrino oscillations I.L.L. experiment reanalysis,” *Appl. Radiat. Isot.* **46**, 449 (1995).
- [40] G. S. Vidyakin, V. N. Vyrodov, I. I. Gurevich, Yu. V. Kozlov, V. P. Martemyanov, S. V. Sukhotin, V. G. Tarasenkov, and S. K. Khakimov, “Detection of Antineutrinos in the Flux From Two Reactors,” *Sov. Phys. JETP* **66**, 243 (1987), [*Zh. Eksp. Teor. Fiz.* 93, 424 (1987)].
- [41] G. S. Vidyakin et al., “Limitations on the characteristics of neutrino oscillations,” *JETP Lett.* **59**, 390 (1994), [*Pisma Zh. Eksp. Teor. Fiz.* 59, 364 (1994)].
- [42] Yu. V. Kozlov, S. V. Khalturtsev, I. N. Machulin, A. V. Martemyanov, V. P. Martemyanov, S. V. Sukhotin, V. G. Tarasenkov, E. V. Turbin, and V. N. Vyrodov, “Antineutrino-Deuteron Experiment at the Krasnoyarsk Reactor,” *Phys. Atom. Nucl.* **63**, 1016 (2000), [*Yad. Fiz.* 63, 1091 (2000)], hep-ex/9912047.
- [43] G. Boireau et al. (NUCIFER), “Online Monitoring of the Osiris Reactor with the Nucifer Neutrino Detector,” *Phys. Rev.* **D93**, 112006 (2016), 1509.05610.
- [44] Z. D. Greenwood et al., “Results of a two position reactor neutrino oscillation experiment,” *Phys. Rev.* **D53**, 6054 (1996).
- [45] A. I. Afonin, S. N. Ketov, V. I. Kopeikin, L. A. Mikaelyan, M. D. Skorokhvatov, and S. V. Tolokonnikov, “A Study of the Reaction $\bar{\nu}_e + P \rightarrow e^+ + N$ on a Nuclear Reactor,” *Sov. Phys. JETP* **67**, 213 (1988), [*Zh. Eksp. Teor. Fiz.* 94 N2,1 (1988)].
- [46] A. A. Kuvshinnikov, L. A. Mikaelyan, S. V. Nikolaev, M. D. Skorokhvatov, and A. V. Etenko, “Measuring the $\bar{\nu}_e + p \rightarrow n + e^+$ cross-section and beta decay axial constant in a new experiment at Rovno NPP reactor. (In Russian),” *JETP Lett.* **54**, 253 (1991), [*Sov. J. Nucl. Phys.* 52, 300 (1990)].
- [47] M. Apollonio et al. (CHOOZ), “Search for neutrino oscillations on a long baseline at the CHOOZ nuclear power station,” *Eur. Phys. J.* **C27**, 331 (2003), hep-ex/0301017.
- [48] F. Boehm et al., “Final results from the Palo Verde neutrino oscillation experiment,” *Phys. Rev.* **D64**, 112001 (2001), hep-ex/0107009.
- [49] G. Gratta, Private Communication.
- [50] F. P. An et al. (Daya Bay), “Evolution of the Reactor Antineutrino Flux and Spectrum at Daya Bay,” *Phys. Rev. Lett.* **118**, 251801 (2017), 1704.01082.
- [51] G. Bak et al. (RENO), “Fuel-composition dependent reactor antineutrino yield and spectrum at RENO,” (2018), 1806.00574.
- [52] S.-B. Kim, Private Communication.
- [53] I. Esteban, M. C. Gonzalez-Garcia, A. Hernández-Cabezudo, M. Maltoni, and T. Schwetz, “Global analysis of three-flavour neutrino oscillations: synergies and tensions in the determination of θ_{23} , δ_{CP} , and the mass ordering,” *JHEP* **01**, 106 (2019), 1811.05487.
- [54] J. Ashenfelter et al. (PROSPECT), “The PROSPECT Physics Program,” *J. Phys.* **G43**, 113001 (2016), 1512.02202.
- [55] S. Gariazzo, C. Giunti, M. Laveder, and Y. F. Li, “Updated Global 3+1 Analysis of Short-BaseLine Neutrino Oscillations,” *JHEP* **06**, 135 (2017), 1703.00860.
- [56] C. Giunti, X. P. Ji, M. Laveder, Y. F. Li, and B. R. Littlejohn, “Reactor Fuel Fraction Information on the Antineutrino Anomaly,” *JHEP* **10**, 143 (2017), 1708.01133.
- [57] M. Dentler, A. Hernández-Cabezudo, J. Kopp, M. Maltoni, and T. Schwetz, “Sterile neutrinos or flux uncertainties? – Status of the reactor anti-neutrino anomaly,” *JHEP* **11**, 099 (2017), 1709.04294.
- [58] C. Giunti, Y. F. Li, B. R. Littlejohn, and P. T. Surukuchi, “Diagnosing the Reactor Antineutrino Anomaly with Global Antineutrino Flux Data,” *Phys. Rev.* **D99**, 073005 (2019), 1901.01807.
- [59] A. C. Hayes, J. L. Friar, G. T. Garvey, G. Jungman, and G. Jonkmans, “Systematic Uncertainties in the Analysis of the Reactor Neutrino Anomaly,” *Phys. Rev. Lett.* **112**, 202501 (2014), 1309.4146.
- [60] I. Alekseev et al. (DANSS), “Search for sterile neutrinos at the DANSS experiment,” *Phys. Lett.* **B787**, 56 (2018), 1804.04046.
- [61] D. Adey et al. (Daya Bay), “Measurement of the Electron Antineutrino Oscillation with 1958 Days of Operation at Daya Bay,” *Phys. Rev. Lett.* **121**, 241805 (2018), 1809.02261.
- [62] F. P. An et al. (Daya Bay), “Improved Measurement of the Reactor Antineutrino Flux and Spectrum at Daya Bay,” *Chin. Phys.* **C41**, 013002 (2017), 1607.05378.
- [63] J. Ashenfelter et al. (PROSPECT), “First search for short-baseline neutrino oscillations at HFIR with PROSPECT,” *Phys. Rev. Lett.* **121**, 251802 (2018), 1806.02784.
- [64] H. Almazán et al. (STEREO), “Sterile Neutrino Constraints from the STEREO Experiment with 66 Days of Reactor-On Data,” *Phys. Rev. Lett.* **121**, 161801 (2018), 1806.02096.
- [65] L. Bernard (STEREO), in *54th Rencontres de Moriond on Electroweak Interactions and Unified Theories (Moriond EW 2019) La Thuile, Italy, March 16-23, 2019* (2019), 1905.11896.
- [66] M. Agostini and B. Neumair, “Statistical Methods for the Search of Sterile Neutrinos,” (2019), 1906.11854.
- [67] J. R. Alonso and K. Nakamura (IsoDAR), “IsoDAR@KamLAND: A Conceptual Design Report for the Conventional Facilities,” (2017), 1710.09325.
- [68] H. T. Wong, “Ultra-Low-Energy Germanium Detector for Neutrino-Nucleus Coherent Scattering and Dark Matter Searches,” *Mod. Phys. Lett.* **A23**, 1431 (2008), 0803.0033.
- [69] D. Yu. Akimov et al. (RED), “Prospects for observation of neutrino-nuclear neutral current coherent scat-

- tering with two-phase Xenon emission detector,” JINST **8**, P10023 (2013), 1212.1938.
- [70] A. Gütlein et al., “Impact of coherent neutrino nucleus scattering on direct dark matter searches based on CaWO_4 crystals,” *Astropart. Phys.* **69**, 44 (2015), 1408.2357.
- [71] V. Belov et al., “The νGeN experiment at the Kalinin Nuclear Power Plant,” JINST **10**, P12011 (2015).
- [72] A. Aguilar-Arevalo et al. (CONNIE), “Results of the engineering run of the Coherent Neutrino Nucleus Interaction Experiment (CONNIE),” JINST **11**, P07024 (2016), 1604.01343.
- [73] G. Agnolet et al. (MINER), “Background Studies for the MINER Coherent Neutrino Scattering Reactor Experiment,” *Nucl. Instrum. Meth.* **A853**, 53 (2017), 1609.02066.
- [74] J. Billard et al., “Coherent Neutrino Scattering with Low Temperature Bolometers at Chooz Reactor Complex,” *J. Phys.* **G44**, 105101 (2017), 1612.09035.
- [75] R. Strauss et al., “The ν -cleus experiment: A gram-scale fiducial-volume cryogenic detector for the first detection of coherent neutrino-nucleus scattering,” *Eur. Phys. J.* **C77**, 506 (2017), 1704.04320.
- [76] D. Akimov et al. (COHERENT), “Observation of Coherent Elastic Neutrino-Nucleus Scattering,” *Science* (2017), 1708.01294.
- [77] J. Hakenmüller, “The CONUS Experiment,” URL https://indico.cern.ch/event/606690/contributions/2591545/attachments/1499330/2336272/Taup2017_CONUS_talk_JHakenmueller.pdf.
- [78] B. C. Cañas, E. A. Garcés, O. G. Miranda, and A. Parada, “The reactor antineutrino anomaly and low energy threshold neutrino experiments,” *Phys. Lett.* **B776**, 451 (2018), 1708.09518.
- [79] C. Blanco, D. Hooper, and P. Machado, “Constraining Sterile Neutrino Interpretations of the LSND and Mini-BooNE Anomalies with Coherent Neutrino Scattering Experiments,” (2019), 1901.08094.